



## Structure and magnetic properties of $Gd_xY_{1-x}FeO_3$ obtained by mechanosynthesis



A.M. Bolarín-Miró<sup>a,\*</sup>, F. Sánchez-De Jesús<sup>a,\*</sup>, C.A. Cortés-Escobedo<sup>b</sup>, R. Valenzuela<sup>c</sup>, S. Ammar<sup>d</sup>

<sup>a</sup>Área Académica de Ciencias de la Tierra y Materiales, Universidad Autónoma del Estado de Hidalgo Mineral de la Reforma, Hidalgo 42184, Mexico

<sup>b</sup>Centro de Investigación e Innovación Tecnológica del IPN, Distrito Federal 02250, Mexico

<sup>c</sup>Depto. de Materiales Metálicos y Cerámicos, Instituto de Investigaciones en Materiales, Universidad Nacional Autónoma de México, México D.F. 04510, Mexico

<sup>d</sup>ITODYS, UMR 7086, Université de Paris-Diderot, 75250 Paris Cedex, France

### ARTICLE INFO

#### Article history:

Available online 13 April 2013

#### Keywords:

Mechanochemistry  
Orthoferrite  
Doped  $GdFeO_3$   
Doped  $YFeO_3$   
Mechanochemical processing

### ABSTRACT

Solid solutions of yttrium–gadolinium orthoferrites  $Gd_xY_{1-x}FeO_3$  ( $0 \leq x \leq 1$ ) were prepared by high-energy ball milling. The aim of this work was to study the influence of the synthesis parameters on the crystal structure and the magnetic behavior of these solid solutions. The precursors,  $Fe_2O_3$ ,  $Y_2O_3$  and  $Gd_2O_3$ , mixed in a stoichiometric ratio to obtain these orthoferrites, were milled for different times (up to 5 h). X-ray diffraction and Rietveld refinement were used to elucidate the phase transformation as a function of the milling time. Results showed the complete formation of orthoferrite with an orthorhombic structure (S.G. *Pbnm*) without any annealing after 5 h of milling for all of the compositions. The effect of the synthesis process and the  $x$  value on the crystal structure and the magnetic properties were also studied. All of the synthesized powders demonstrated weak ferromagnetic behavior. In particular, an increase in the maximum magnetization for all the compositions was found, with a maximum that reached 7.7 emu/g for  $Gd_{0.75}Y_{0.25}FeO_3$ . For  $Gd_{0.5}Y_{0.5}FeO_3$ , the magnetization decreases down to 2.1 emu/g. A small contamination of metallic Fe was confirmed through electron spin resonance experiments.

© 2013 Elsevier B.V. All rights reserved.

### 1. Introduction

Ceramics with a perovskite structure have been a subject of interest for researchers due to their potential technological applications [1,2]. In particular, yttrium orthoferrite,  $YFeO_3$ , and its related solid solutions (substituted orthoferrites) are among a wide variety of functional materials that are used in many electronic applications and are attractive materials for use in other applications, such as in the memory elements of logic devices in computer engineering, as well as for use in catalysis, gas separation systems, cathodes of solid oxide fuel cells, sensors, magneto-optical systems, magnetic field sensors and information recording and storage systems [2–5].

Rare earth orthoferrites,  $RFeO_3$ , where  $R$  is the rare earth, crystallize in the perovskite structure [6], with the  $Fe^{3+}$  ion surrounded by six oxygen ions in the B-sites [7] and with  $R$  in the A-sites.  $YFeO_3$ , which is weakly ferromagnetic due to a canted antiferromagnetic structure [8], presents a polymorphic behavior and crystallizes in either orthorhombic or hexagonal structures, depending on the synthesis conditions [9].

When magnetic  $Gd^{3+}$  is partially substituted for non-magnetic  $Y^{3+}$  in  $YFeO_3$ , the generation of new magnetic interactions [10] and the ensuing changes in the material's magnetic behavior are expected. The incorporation of a bigger cation, such as substituting  $Gd^{3+}$  (ionic radii 0.938 Å) for  $Y^{3+}$  (ionic radii 0.90 Å) into the  $YFeO_3$  structure in the A sites, increases the Goldschmidt's tolerance factor, presumably helping to induce variations in the lattice parameters with respect to the *Pbnm* structure that is found at lower  $Gd^{3+}$  concentrations. This structural change or distortion of the crystal structure should modify the magnetic behavior of the ceramic [11].

To obtain orthoferrites, several synthesis methods have been developed [12–16]. The mechanochemical process (MCP) is an effective, economical and versatile way to produce  $RFeO_3$  using powder oxide mixtures. The effectiveness of the high-energy ball milling technique to promote the mechanosynthesis of the nanostructured ferrites by the mechanical activation of oxide compounds has been shown to yield excellent results [17–20] for diverse types of orthoferrites, such as  $YFeO_3$  [21],  $LaFeO_3$  [22],  $La_{1-x}Y_xFeO_3$  [11],  $Ca_{1-x}La_xFeO_3$  [23] and  $Bi_{1-x}Y_xFeO_3$  [24]. To the best of our knowledge, there are no references about the use of this technique to obtain solid solutions of  $Gd_{1-x}Y_xFeO_3$  orthoferrites. Because in this process the magnetic ion is incorporated into the

\* Corresponding author. Tel.: +52 7717172000x2280.

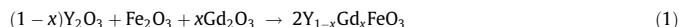
E-mail address: [fsanchez@uaeh.edu.mx](mailto:fsanchez@uaeh.edu.mx) (F. Sánchez-De Jesús).

lattice, a change in the magnetic properties when compared to the parent material is expected.

The aim of this work was to demonstrate that MCP induces the formation of nanostructured  $\text{Gd}_{1-x}\text{Y}_x\text{FeO}_3$  with a perovskite-like structure by mechanosynthesis without the need of a heat treatment. We also report the effects of synthesis parameters on the magnetic properties of the mixed yttrium–gadolinium orthoferrite.

## 2. Experimental procedure

$\text{Fe}_2\text{O}_3$  (Sigma Aldrich, 99% purity),  $\text{Gd}_2\text{O}_3$  (Sigma Aldrich, 99% purity) and  $\text{Y}_2\text{O}_3$  (Sigma Aldrich, 99.9% purity) reagent powders were used as precursor materials. These powders were mixed in a stoichiometric ratio according to the following equation:



A total of 5 g of the starting mixture as well as steel balls with a diameter of 1.27 cm were loaded into a steel cylindrical vial (50 cm<sup>3</sup>) (steel/steel, S/S) at room temperature and milled for different times, up to 5 h, using an SPEX 8000D mixer/mill. The ball to powder weight ratio was 10:1. The experimental parameters utilized in this study were developed in previous studies [25]. All of the experiments were performed in an atmosphere of air.

The milled powders were characterized by X-ray diffraction (XRD) using a Siemens D5000 diffractometer with  $\text{Co K}\alpha_1$  ( $\lambda = 1.7889 \text{ \AA}$ ) radiation. Patterns were collected in a  $2\theta$  interval of  $10\text{--}100^\circ$  with increments of  $0.02$  ( $2\theta$ ). Rietveld refinement was performed on the X-ray patterns. This refinement method takes all of the information collected in a pattern and utilizes a least squares approach method to refine the theoretical line profile until it matches the measured profile. The lattice parameters of the powder and the microstrain were obtained from the XRD line positions using a refinement method [26]. The magnetization studies were performed at room temperature using a MicroSense V7 vibrating sample magnetometer with a maximum field of 18 kOe. The electron spin resonance (ESR) experiments were carried out at room temperature and at a frequency of 9.43 GHz (X-band) in a Miniscope 400, by Magnettech GmbH Germany.

## 3. Results and discussion

Fig. 1 shows the X-ray diffraction patterns of mixtures of  $\text{Fe}_2\text{O}_3$  and  $\text{Y}_2\text{O}_3$  to obtain  $\text{YFeO}_3$  ( $x = 0$ ), after different milling times, up to 5 h. The XRD pattern corresponding to the mixture of the unmilled precursor powders confirms the peaks of the starting materials:  $\text{Fe}_2\text{O}_3$  (ICDS #43465) and  $\text{Y}_2\text{O}_3$  (ICDS #78581). Mechanosynthesis performed for 1 h clearly exhibits peaks of yttrium orthoferrite,  $\text{YFeO}_3$  (ICDS #43260, orthoferrite), which is demonstrated by the main peak located at approximately  $2\theta = 38.6^\circ$ . Simultaneously, peaks belonging to the original oxides vanished, with the exception of the main peak belonging to  $\text{Y}_2\text{O}_3$  (at approximately  $2\theta = 34^\circ$ ). The amount of  $\text{YFeO}_3$  increased with milling time, as was observed for the mixtures milled for 3 and 5 h. The pattern of the 5 h milled

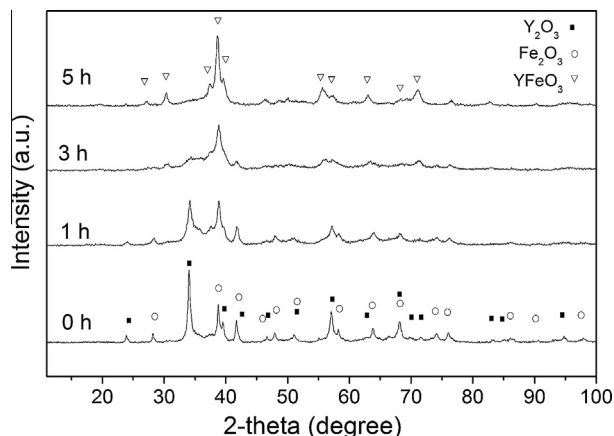


Fig. 1. X-ray powder diffraction patterns of the mixture of oxides ( $\text{Fe}_2\text{O}_3$  and  $\text{Y}_2\text{O}_3$ ) in order to obtain  $\text{YFeO}_3$  milled at various times, up to 5 h.

sample shows no peaks belonging to the starting materials, indicating that the reaction given by Eq. (1) was completed. The mechanosynthesis of yttrium orthoferrite starts in the first hour of milling and is completed after 5 h. As expected during the milling process, a remarkable broadening of the peak profile occurs due to crystallite size reduction and lattice strain promoted by the milling process [27].

Fig. 2 presents the XRD patterns of the different mixtures of  $\text{Fe}_2\text{O}_3$ ,  $\text{Gd}_2\text{O}_3$  and  $\text{Y}_2\text{O}_3$  that were milled for 5 h to obtain  $\text{Gd}_x\text{Y}_{1-x}\text{FeO}_3$ , with  $x$  varying from 0 to 1. The obtained results confirm that in all of the compositions, the formation of solid solutions of yttrium–gadolinium ferrites with a perovskite-like orthorhombic (space group  $Pbnm$ ) structure ( $\text{Gd}_x\text{Y}_{1-x}\text{FeO}_3$ , orthoferrite) is completed after 5 h, as evidenced by the absence of peaks other than those belonging to the  $Pbnm$  space group. This result is in agreement with the previous results presented in Fig. 1 for yttrium orthoferrite ( $x = 0$ ).

The amplification of the XRD pattern about  $2\theta \sim 39^\circ$  shows a shift of the main diffraction peak toward lower angle values (i.e., a larger unit cell) as  $x$  is increased. This change can be associated with the slightly larger ionic radii of  $\text{Gd}^{3+}$  (ionic radii  $0.938 \text{ \AA}$  in coordination VI) compared with the substituted  $\text{Y}^{3+}$  (ionic radii  $0.90 \text{ \AA}$  in coordination VI) [28].

Rietveld refinement was performed using the XRD patterns shown in Fig. 2. Table 1 presents some parameters of the goodness of fit ( $R_{wp}$ ,  $R_p$ ,  $\chi^2$ ), and Fig. 3 presents a typical diffraction pattern of the results of the Rietveld refinement of mixtures of  $\text{Fe}_2\text{O}_3$  and  $\text{Y}_2\text{O}_3$  that were milled for 5 h in order to obtain  $\text{YFeO}_3$ ; both of these figures suggest a high quality fit of the data with the refinement. This refinement was used to calculate the r.m.s. microstrain, cell parameter, and crystallite size and the unit cell volume of the obtained orthoferrites.

Results for the r.m.s. microstrain and  $a$  cell parameter are shown in Fig. 4; here, a consistent increment in the cell parameter with the increase in the amount of gadolinium, from  $5.2958 \pm 0.0013 \text{ \AA}$  to  $5.3354 \pm 0.0008 \text{ \AA}$  (from  $x = 0$  to 1, respectively) is apparent, as a consequence of the different ionic radii. After analyzing the results of r.m.s. microstrain shown in Fig. 4 together with the XRD patterns, it was observed that the lattice distortion was promoted by the presence of ions with different radii that changed the symmetry of the cell without changing the  $Pbnm$  space group. This result is in agreement with the calculation of the Goldschmidt's tolerance factor of  $\text{Gd}_x\text{Y}_{1-x}\text{FeO}_3$ , which is 0.85 and 0.84 for  $x = 1$  and  $x = 0$ , respectively, if a coordination of VIII is assumed for the calculus (ionic radii of  $\text{Y}^{3+}$  and  $\text{Gd}^{3+}$   $1.019 \text{ \AA}$  and  $1.053 \text{ \AA}$ , respectively [28]); both of these values are within the known range of Goldschmidt's tolerance factor for orthorhombic structures ( $<1$ ) [29]. Although there is a stabilization of the orthorhombic structure, the mechanochemical process used for the synthesis, in combination with the presence of the different number of gadolinium cations in all of the compositions except for the composition of  $x = 0.5$ , promote an increase of the microstrain in the cell (with respect to the same cell synthesized by chemical methods). For the composition of  $\text{Gd}_{0.5}\text{Y}_{0.5}\text{FeO}_3$ , the stabilization of the r.m.s. microstrain may be a consequence of the equivalent amounts of  $\text{Gd}^{3+}$  and  $\text{Y}^{3+}$  ions that help to decrease the internal stresses.

Fig. 5 shows the magnetic hysteresis loops for  $\text{YFeO}_3$  as a function of milling time. The initial mixture (milling time of 0 h) shows a very small value of magnetization ( $1.2 \text{ emu/g}$ ), which can be associated with the magnetic behavior of the  $\text{Fe}_2\text{O}_3$  (weak ferromagnetic) and  $\text{Y}_2\text{O}_3$  (diamagnetic) precursors [30]. Increasing the milling time to 1 h has little effect on the magnetization because the synthesis of the orthoferrite has just started. The value of magnetization of the sample increases to  $\sim 3.8 \text{ emu/g}$  after 3 h of milling time and  $\sim 4 \text{ emu/g}$  after 5 h of milling time. According to XRD,

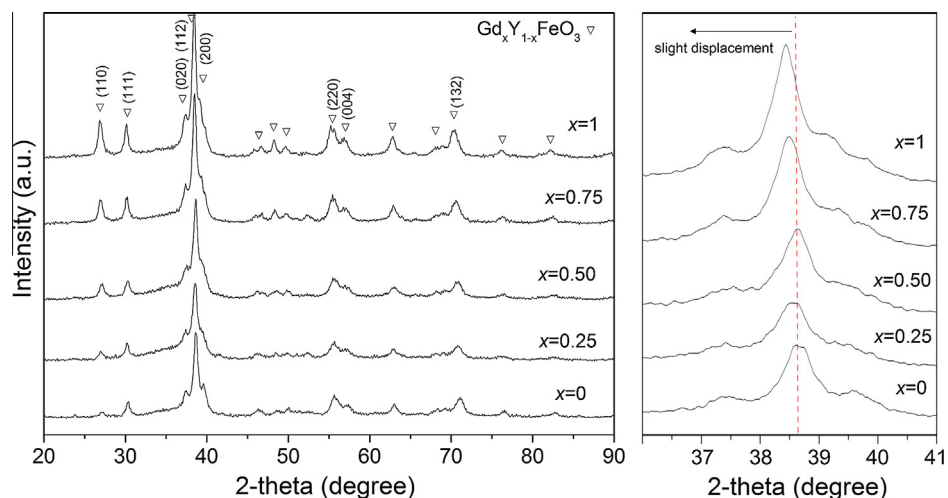


**Fig. 2.** XRD patterns of the series of activated samples for the different compositions of  $\text{Y}_{1-x}\text{Gd}_x\text{FeO}_3$  ( $0 \leq x \leq 1$ ) milled for 5 h. The shift of the main diffraction peak is a result of the substitution of  $\text{Y}^{3+}$  by  $\text{Gd}^{3+}$  and is shown in detail on the right.

**Table 1**

Cell parameters, volume of the unit cell and crystal size for the  $Pbnm$  structure, as well as the Rietveld refinement parameters.

| Composition ( $x$ ) | Cell parameters         |                         |                         | Crystallite size (Å) | Unit cell volume (Å <sup>3</sup> ) | Goodness of fit |       |                  |
|---------------------|-------------------------|-------------------------|-------------------------|----------------------|------------------------------------|-----------------|-------|------------------|
|                     | $a$ (Å)                 | $b$ (Å)                 | $c$ (Å)                 |                      |                                    | $\chi^2$        | $R_w$ | $R_{\text{exp}}$ |
| 0                   | 5.2958 ( $\pm 0.0013$ ) | 5.6028 ( $\pm 0.0015$ ) | 7.6410 ( $\pm 0.0020$ ) | 187.4 ( $\pm 2.84$ ) | 226.72 ( $\pm 4 \times 10^{-10}$ ) | 1.338           | 20.37 | 17.61            |
| 0.25                | 5.3035 ( $\pm 0.0017$ ) | 5.6520 ( $\pm 0.0018$ ) | 7.6452 ( $\pm 0.0032$ ) | 148.4 ( $\pm 1.85$ ) | 229.17 ( $\pm 1 \times 10^{-10}$ ) | 1.495           | 19.66 | 16.08            |
| 0.50                | 5.3196 ( $\pm 0.0017$ ) | 5.6178 ( $\pm 0.0019$ ) | 7.6575 ( $\pm 0.0030$ ) | 153.0 ( $\pm 1.83$ ) | 228.84 ( $\pm 4 \times 10^{-10}$ ) | 1.226           | 11.16 | 10.08            |
| 0.75                | 5.3334 ( $\pm 0.0009$ ) | 5.6062 ( $\pm 0.0009$ ) | 7.6746 ( $\pm 0.0014$ ) | 208.3 ( $\pm 0.75$ ) | 229.47 ( $\pm 1 \times 10^{-9}$ )  | 1.401           | 11.31 | 9.54             |
| 1                   | 5.3354 ( $\pm 0.0008$ ) | 5.5958 ( $\pm 0.0007$ ) | 7.6557 ( $\pm 0.0009$ ) | 215.1 ( $\pm 1.27$ ) | 228.57 ( $\pm 5 \times 10^{-10}$ ) | 1.025           | 12.01 | 11.86            |

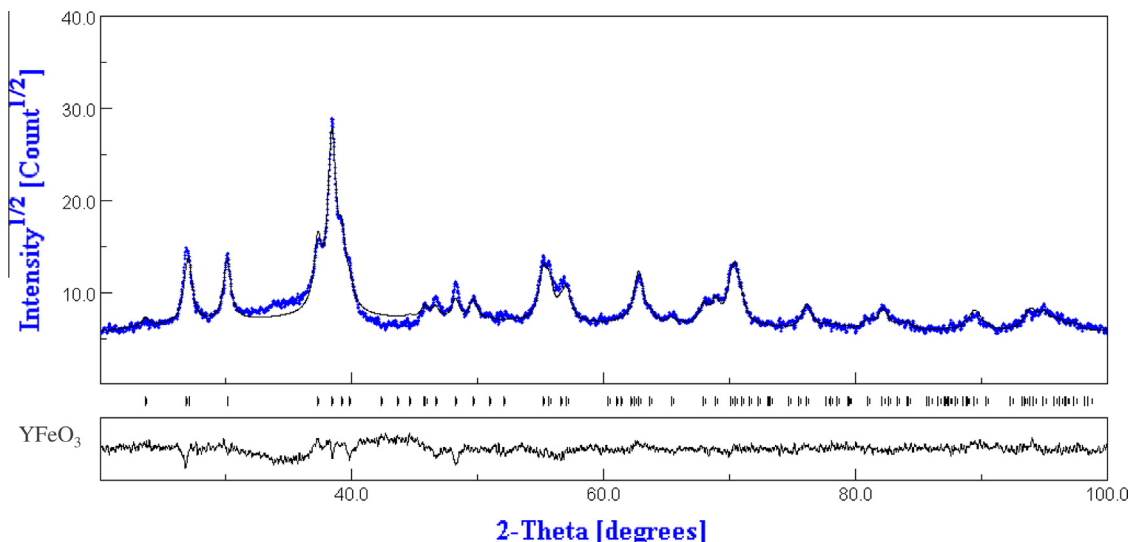


**Fig. 3.** Rietveld refinement of an X-ray powder diffraction pattern of the mixture of  $\text{Y}_2\text{O}_3$  and  $\text{Fe}_2\text{O}_3$  milled for 5 h in order to obtain  $\text{YFeO}_3$ .

the synthesis of the orthoferrite has been completed by this milling time.  $\text{YFeO}_3$  is a canted antiferromagnet, with magnetization of approximately 0.2 emu/g [31]. Apparently, the large magnetic moment is attributed to the formation of a small amount of ferro- or ferromagnetic precipitation that was not detected by XRD. The coercive field and saturation magnetization for all of the studied compounds for the milling time of 5 h are displayed in Table 2 and are presented in Fig. 6. Current literature reports a magnetization value of 0.2 emu/g for  $\text{YFeO}_3$  and 2.2 emu/g for  $\text{GdFeO}_3$  [8,31–32], which again suggests that some contamination of the expected

compounds is present and similar in origin to the contamination seen with  $\text{YFeO}_3$ .

In order to assess the contamination, measurements of the electron spin resonance (ESR) in the X band (9.43 GHz) were carried out at room temperature for the  $x = 1$  series ( $\text{GdFeO}_3$  as the end product) and shown in Fig. 7. These materials exhibited a magnetic hysteresis behavior very similar to that of  $\text{YFeO}_3$ . For the starting materials (no milling), a broad resonance was observed and associated with hematite [33]. For 3 h of milling time, a clear change in the resonance signal was observed; this result is significantly

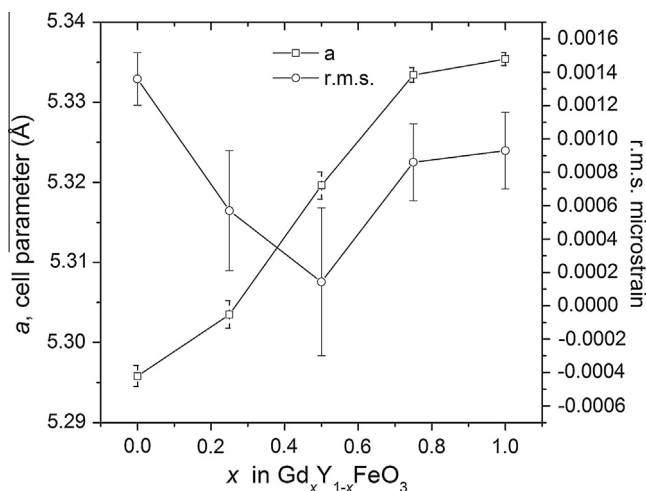


Fig. 4. Cell parameter (a) and r.m.s. microstrain of  $Gd_xY_{1-x}FeO_3$  ( $0 \leq x \leq 1$ ).

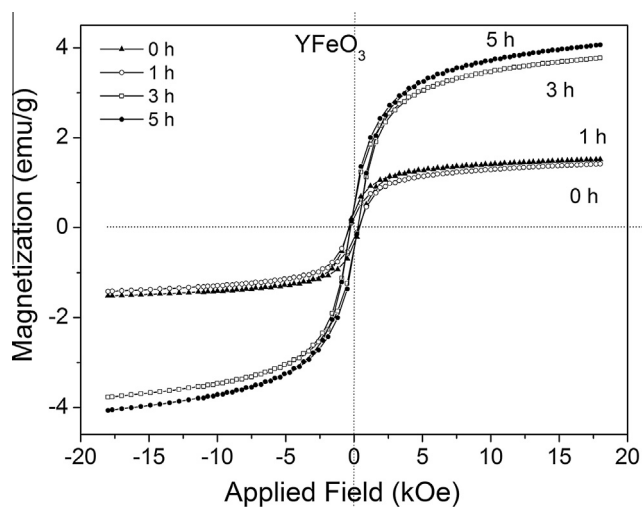


Fig. 5. Magnetic hysteresis loop for mixtures of  $Fe_2O_3$  and  $Y_2O_3$  milled for different times (0–5 h) to obtain  $YFeO_3$ .

Table 2

Magnetic properties ( $H_c$ : coercivity and  $M_s$ : saturation magnetization) for mixtures of  $Fe_2O_3$  and  $Y_2O_3$  milled for 5 h to obtain different compositions of  $Gd_xY_{1-x}FeO_3$  ( $0 \leq x \leq 1$ ).

| Composition (x) | $Gd_xY_{1-x}FeO_3$ formula | $H_c$ (kOe) | $M_s$ (emu/g) |
|-----------------|----------------------------|-------------|---------------|
| 0               | $YFeO_3$                   | 0.2783      | 4.05          |
| 0.25            | $Gd_{0.25}Y_{0.75}FeO_3$   | 0.1176      | 6.79          |
| 0.5             | $Gd_{0.5}Y_{0.5}FeO_3$     | 0.1765      | 2.76          |
| 0.75            | $Gd_{0.75}Y_{0.25}FeO_3$   | 0.1535      | 7.72          |
| 1               | $GdFeO_3$                  | 0.1861      | 4.59          |

amplified after milling for 5 h. The latter spectrum corresponds to the ferromagnetic resonance of metallic iron [34]. The resonance field is very low due to the strong internal field of metallic iron; in order to fulfill the resonance conditions of the Larmor equation, when the strong internal field of the metallic iron is added to the total field, the applied resonance field is strongly decreased. This signal also rules out the possibility of magnetite as a contaminant, as magnetite has a ferromagnetic resonance frequency of approximately 3.5 kOe at room temperature [35]. It is important to note that the ESR experiments are extremely sensitive to ferromagnetic materials. As demonstrated below, it can be estimated that a con-

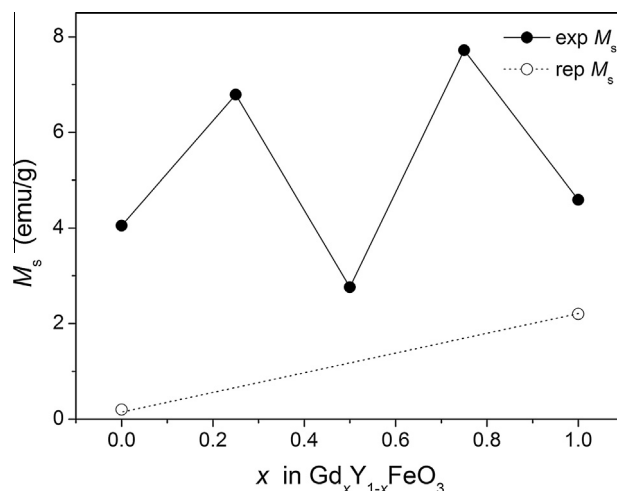


Fig. 6. Magnetization as a function of composition  $x$ , for samples milled for 5 h (experimental  $M_s$  represented by full circles). Open circles show the reported values [8,31,32] for the end products.

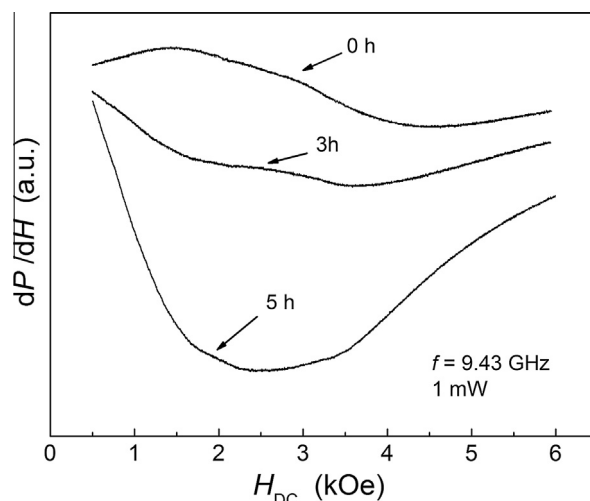


Fig. 7. Electron spin resonance of a mixture of  $Fe_2O_3$  and  $Gd_2O_3$  without milling (reagents mixture), milled for 3 h, and milled for 5 h.

tamination of less than 2 wt% can completely change the observed signal, especially if the other phases in the material are not ferromagnetic, which is the case in these experiments.

If a simple addition effect between magnetic phases is assumed, the iron contamination can be estimated as:

$$M_T = yM_{YFeO_3} + (1 - y)M_{Fe} \quad (2)$$

where  $M_T$  is the total magnetization,  $y$  is the  $YFeO_3$  concentration fraction with a magnetization  $M_{YFeO_3}$  ( $\sim 0.2$  emu/g),  $(1 - y)$  is the metallic iron content and  $M_{Fe}$  is its magnetization (217.2 emu/g). The result is  $y \approx 1.8$  wt%, which is below the XRD detection limit.

In Fig. 6 the expected values for the end products, 0.2 emu/g for  $YFeO_3$  and 2.2 emu/g for  $GdFeO_3$  [8,31,32] were added on top of our experimental results (for samples milled for 5 h). The mean magnetization slope is very close to that for the linear increase in literature values. Thus, in some way, the increase of magnetization with respect to this line is a representation of the contamination in the obtained orthoferrites. In Fig. 6, the clear minimum in the magnetization for  $x = 0.5$  is visible. Naturally, this minimum may be linked to Fe precipitation, i.e. the equivalent content of  $Fe^{3+}$  and

Gd<sup>3+</sup> cations may decrease the amount of precipitated Fe. This is an interesting result on its own and should be studied separately.

Although the precipitation of Fe has been proven by our results, some other explanation of the similar effect of the large magnetic moment has recently been proposed. Yuan et al. [10] have reported the effect of Gd<sup>3+</sup> substitution on the magnetic properties of orthoferrites, using a solid state reaction as the method to obtain the material. They suggest that the substitution of Y<sup>3+</sup> ions by Gd<sup>3+</sup> ions effectively enhances the magnetization of YFeO<sub>3</sub> (the increase in the magnetization value to 7.5 emu/g) as a result of the new Gd–Gd and Gd–Fe interactions and the variation of the Fe–O–Fe superexchange bond caused by a distortion of the crystal structure. Apparently, additional studies are needed to elucidate this important phenomenon.

#### 4. Conclusions

Gadolinium–yttrium orthoferrite solid solutions, Gd<sub>1-x</sub>Y<sub>x</sub>FeO<sub>3</sub>, were successfully synthesized by a mechano-synthesis process involving high energy ball milling of Y<sub>2</sub>O<sub>3</sub>, Gd<sub>2</sub>O<sub>3</sub> and Fe<sub>2</sub>O<sub>3</sub>. A ball to powder weight ratio of 10:1 was used. The reaction was completed after 5 h of milling, and no subsequent thermal treatment was needed. The lattice of the orthoferrite obtained was orthorhombic for all of the compositions (S.G. *Pbnm*). All of the synthesized powders demonstrated a weak ferromagnetic behavior. The magnetization, under a maximum field of 18 kOe, increased from 4 emu/g for YFeO<sub>3</sub> to 7.7 emu/g for Gd<sub>0.75</sub>Y<sub>0.25</sub>FeO<sub>3</sub>. A minimum value of 2.1 emu/g was observed for *x* = 0.5. The differences in expected and measured magnetizations can be attributed to the magnetic-ion substitution at the Y-site by a magnetic ion (Gd<sup>3+</sup>) and a small contamination of iron during milling, which was demonstrated through ESR experiments.

#### Acknowledgments

This project was financially assisted by the National Science and Technology Council of Mexico, CONACyT, under Grants Nos. 129910, 130413 and ANR-CONACyT 139292. Authors would like to acknowledge the technical contribution with the X-ray diffraction measurements from Adriana Tejeda-Cruz.

#### References

[1] M. Rajendran, A.K. Bhattacharya, J. Eur. Ceram. Soc. 26 (2006) 3675–3679.

- [2] A. Bhalla, R.S. Guo, R. Roy, Mater. Res. Innovations 4 (2000) 3–26.  
 [3] A.R. Akbashev, A.S. Semisalova, N.S. Perov, A.R. Kaul, Appl. Phys. Lett. 99 (2011) 122502–122504.  
 [4] Y. Zhang, J. Yang, J. Xu, Q. Gao, Z. Hong, Mater. Lett. 81 (2012) 1–4.  
 [5] M.A. Gillo, J. Chem. Phys. 24 (1956) 1239–1243.  
 [6] S. Mathur, H. Shen, N. Leckerf, A. Kjekshus, H. Fjellvag, C.F. Goya, Adv. Mater. 14 (2002) 1405–1409.  
 [7] A.A. Cristóbal, P.M. Botta, P.G. Bercoff, E.F. Anglietti, H.B. Bertorello, J.M. Porto-López, J. Alloys Comp. 495 (2010) 516–519.  
 [8] H. Shen, J. Xu, A. Wu, J. Zhao, M. Shi, Mater. Sci. Eng. B 157 (2009) 77–80.  
 [9] A. Wu, H. Shen, J. Xu, L. Jiang, L. Luo, S. Cao, H. Zhang, J. Sol–Gel Sci. Technol. 59 (2011) 158–163.  
 [10] Xueping Yuan, Yue Sun, Xu Mingxiang, J. Solid State Chem. 196 (2012) 362–366.  
 [11] A.A. Cristóbal, P.M. Botta, E.F. Anglietti, S. Conconi, P.G. Bercoff, J.M. Porto López, Mater. Chem. Phys. 130 (2011) 1275–1279.  
 [12] J.B. Smith, T. Norby, Solid State Ionics 177 (7–8) (2006) 639–646.  
 [13] A.D. Jadhav, A.B. Gaikwad, V. Samuel, V. Ravi, Mater. Lett. 61 (10) (2007) 2030–2032.  
 [14] C. Matei, D. Berger, S. Stoleriu, F. Papa, V. Fruth, J. Optoelectron. Adv. Mater. 9 (2007) 1793–1796.  
 [15] D.M. Gil, M.C. Navarro, M.C. Lagarrigue, J. Guimpel, R.E. Carbonio, M.I. Gómez, J. Therm. Anal. Calorim. 103 (2011) 889–896.  
 [16] M. Popa, J.M. Calderón Moreno, J. Alloys Comp. 509 (2011) 4108–4116.  
 [17] A.M. Bolarín-Miró, P. Vera-Serna, F. Sánchez-De Jesús, C.A. Cortés-Escobedo, J. Mater. Sci.: Mater. Electron. 22 (2011) 1046–1052.  
 [18] P. Sharma, R.A. Rocha, S.N. Medeiros, A. Paesano Jr., J. Alloys Comp. 443 (2007) 37–42.  
 [19] L.J. Berchmans, M. Myndyk, K.L. Da Silva, A. Feldhoff, J. Šubrt, P. Heitjans, K.D. Becker, V. Šepelák, J. Alloys Comp. 500 (2010) 68–73.  
 [20] M. Algueró, J. Ricote, T. Hungria, A. Castro, Chem. Mater. 19 (2007) 4982–4990.  
 [21] V. Berbenni, C. Milanese, G. Bruni, A. Girella, A. Marini, Thermochim. Acta 521 (2011) 218–223.  
 [22] A.A. Cristóbal, P.M. Botta, P.G. Bercoff, J.M. Porto López, Mater. Res. Bull. 44 (2009) 1036–1040.  
 [23] G. Pecchi, P. Reyes, R. Zamora, C. Campos, L.E. Cadus, B.P. Barbero, Catal. Today 133 (2008) 420–427.  
 [24] Wu. Yu-jie, J. Magn. Mater. 324 (2012) 1348–1352.  
 [25] F. Sánchez-De Jesús, C.A. Cortés-Escobedo, R. Valenzuela, S. Ammar, A.M. Bolarín-Miró, Ceram. Int. 38 (2012) 5257–5263.  
 [26] D. Balzar, N.C. Popa, Rigaku J. 22 (2005) 16–25.  
 [27] A. Moure, A. Castro, J. Tartaj, C. Moure, Ceram. Int. 35 (2009) 2659–2665.  
 [28] R.D. Shannon, Acta Crystallogr. A 32 (1976) 751–767.  
 [29] Hui Shen, Jiayue Xu, Min Jin, Guojian Jiang, Ceram. Int. 38 (2012) 1473–1477.  
 [30] F. Bødker, M.F. Hansen, C. Bender Koch, K. Lefmann, S. Mørup, Phys. Rev. B 61 (2000) 6826–6838.  
 [31] R. Medek, P. Fulmek, J. Nicolics, G.A. Reider, Demagnetizing experiments of yttrium orthoferrites for large aperture magneto optical switch, 31st International Spring Seminar on Electronics Technology, vol. 1, IEEE, 2008, pp. 249–254.  
 [32] Hui. Shen, Xu. Jiayue, Wu. Anhua, J. Rare Earths 28 (2010) 416–419.  
 [33] F.J. Owens, J. Magn. Mater. 321 (2009) 2386–2391.  
 [34] Z. Frait, H. MacFaden, Phys. Rev. 139 (1965) A1173–A1181.  
 [35] J. Kind, U.J. van Raden, I. Garcia-Rubio, A.U. Gehring, Geophys. J. Int. 191 (2012) 51–63.